ACS APPLIED MATERIALS & INTERFACES

Research Article

www.acsami.org

Tailor-Made Hollow Silver Nanoparticle Cages Assembled with Silver Nanoparticles: An Efficient Catalyst for Epoxidation

S. Anandhakumar,*[,†] M. Sasidharan,[†,‡] Cheng-Wen Tsao,[§] and Ashok M. Raichur[∥,⊥]

[†]SRM Research Institute, SRM University, Kattankulathur, Chennai 603 203, Tamil Nadu, India

[‡]Department of Chemistry, Faculty of Science and Engineering, Saga University, 1 Honjo-machi, Saga 840-8502, Japan

[§]Department of Applied Cosmetology, Taoyuan Innovation Institute of Technology, Chungli 32091, Taiwan

[∥]Department of Materials Engineering, Indian Institute of Science, Bangalore 560012, Karnataka, India

[⊥]Department of Applied Chemistry, University of Johannesburg, Doornfontein, Johannesburg 2018, South Africa

Supporting Information

ABSTRACT: A novel approach toward the synthesis of hollow silver nanoparticle (NP) cages built with building blocks of silver NPs by layer-by-layer (LbL) assembly is demonstrated. The size of the NP cage depends on the size of template used for the LbL assembly. The microcages showed a uniform distribution of spherical silver nanoparticles with an average diameter of 20 ± 5 nm, which increased to 40 ± 5 nm when the $AgNO_3$ concentration was increased from 25 to 50 mM. Heat treatment of the polyelectrolyte capsules at 80 °C near their pK_a values yielded intact nano/micro cages. These cages produced a higher conversion for the epoxidation of olefins and maintained their catalytic activity even after four successive uses. The nanocages exhibited unique and attractive characteristics for metal catalytic systems, thus offering the scope for further development as heterogeneous catalysts.

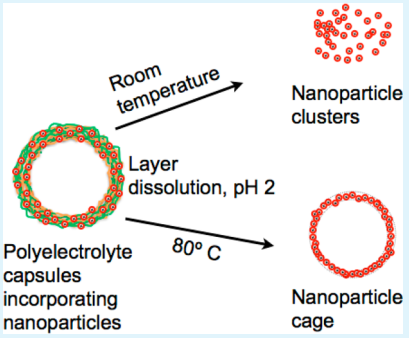

KEYWORDS: *silver NP cages, LbL assembly, catalyst and epoxidation*

1. INTRODUCTION

In recent years, hollow metal NPs (MNPs) have fascinated scientists due to their unique physical and chemical properties such as low density, high surface area, good flow, high surface permeability, and reactivity. MNPs have found wide applications in many fields, such as drug delivery, photonics, catalysis, and energy storage, and conversion devices.[1−4] These properties are largely dependent on their size, morphology, surface architecture, and bulk and surface composition. For instance, MNPs with hollow interiors showed enhanced catalytic activity and were reused several times without any compromise in their catalytic activity.[5] The common preparative method for hollow MNPs is based on the fabrication of core−shell composites using molecular precursors and NPs as inorganic shell building blocks via either a direct surface reaction or precipitation. However, sensitive condensation/polymerization conditions of molecular precursors and the aggregation of NPs complicates the preparation of hollow spheres.[6−10] The other widely used method is the micellar method where La_2O_3 hollow nanospheres were fabricated through the electrostatic interactions between a polystyrene-*b*-poly(acrylic acid)-*b*-polyethylene oxide (PS−PAA−PEO) triblock copolymer with $LaCl_3 \cdot 6H_2O$.[11] The formation of a core−shell-corona micelle in the alkaline region gave La_2O_3 hollow nanospheres after calcination at 550 °C. Preformed vesicles could also be used as templates for fabricating stable gold hollow spheres.[12] NPs were deposited on the vesicle surface either by the direct coating of the nanocolloid or by the reduction of metal ions from the precursors which resulted in hollow vesicle cages incorporating NPs.[12] It was also reported that the direct mixing of metal precursors with Bu_4NBr yields MNP hollow spheres, technically called "metal compound-induced vesicles".[13] This method provides versatility for the fabrication of metal alloy hollow spheres, which consist of more than one MNP. However, the size distribution of the hollow vesicle cages was far from narrow and depended on the metal compound precursors. Furthermore, the presence of layer components might influence and/or interfere with the interactions between the reactants and catalyst surface when used for catalytic applications.

Alternatively, LbL assembly has been demonstrated as a useful technique for the fabrication of hollow structures. It is based on the sequential adsorption of polyelectrolytes onto a charged colloidal template followed by core dissolution. The size of the hollow structure (capsules) depends on the size of the colloidal (sacrificial) template used for LbL assembly. LbL assembly of polyelectrolytes and NPs around polymer particles results in monodisperse Fe_2O_3 or SiO_2 loaded-polymer capsules when the core is selectively removed by calcination or solvent dissolution.[14,15] However, these methods are system specific

Received: November 18, 2013
Accepted: February 19, 2014
Published: February 19, 2014

   dx.doi.org/10.1021/am500229v | ACS Appl. Mater. Interfaces 2014, 6, 3275−3281

and are more successful for metal oxides than for noble metals like silver and gold. To avoid this limitation, we directly synthesized silver NPs in polyelectrolyte capsules by the so-called polyol reduction method.[16] However, obtaining metal nanocages with a particular arrangement/orientation in the shell has not yet been achieved. To the best of our knowledge, the removal of layer components for the fabrication of MNPs cages by LbL assembly has not been reported. Notably, the absence of layer components might provide a higher conversion and yield in catalytic applications. Herein, we report a simple approach to fabricate nanopatterned hollow silver NP cages by the selective leaching of layer constituents in LbL-assembled hollow capsules.

2. EXPERIMENTAL SECTION

2.1. Materials. Dextran sulfate (DS) (MW = 500 kDa), poly(allylamine hydrochloride) (PAH) (MW = 70 kDa), poly-(ethylene glycol) (PEG) (MW = 6 kDa), hydrofluoric acid (HF), ammonium fluoride, anhydrous *tert*-butylhydroperoxide (TBHP), and silver nitrate are commercially available and were purchased from Sigma-Aldrich. All chemicals were used without further purification. Monodisperse silica microparticles with a mean diameter of 4.27 ± 0.25 μm were obtained from Microparticles GmbH (Germany). Milli-Q water with a resistivity greater than 18 MΩ cm was used for all experiments. All pH adjustments were done with 0.1 M HCl or 0.1 M NaOH.

2.2. Synthesis of Silica NPs. Silica NPs were prepared by the hydrolysis of tetraethyl orthosilicate (TEOS) in ethanol in the presence of ammonium hydroxide.[17] Briefly, 0.1 M of TEOS in ethanol was ultrasonicated in a bath reactor. After 20 min, 28% ammonium hydroxide was added as a catalyst to promote the condensation reaction. Sonication was continued for another 60 min to obtain a white turbid suspension of silica NPs. Then the particles were washed with water and used for LbL assembly.

2.3. Capsule Preparation. Nano/microcapsules were prepared by the LbL technique using silica particles as sacrificial templates. The silica particles (1% w/w) were alternatively coated at pH 5 by incubation in 1 mg/mL PAH and DS. The polymer solutions were prepared with 0.2 M NaCl. After adsorption for 15 min, the coated particles were separated by centrifugation and residual polyelectrolyte was removed by washing three times with water (pH 5). After four bilayers were deposited, the silica core was dissolved in 0.1 M HF buffer (0.1 M HF:0.5 M NH_4F) and the obtained capsules were washed and stored in water.

2.4. Fabrication of Multilayer Capsules Incorporating Silver NPs. The fabrication of multilayer capsules incorporating silver NPs involved the sequential adsorption of three layers of PAH and DS on silica micro/NPs, followed by silver NP synthesis.[16] $AgNO_3$ was used as the precursor for the formation of silver NPs. The reduction was performed at 50 °C in the presence of PEG. After the synthesis of the silver NPs, the coated particles were washed and deposited with another bilayer of PAH and DS. Then the silica core was dissolved with HF buffer to obtain the silver NP-incorporated hollow capsules.

2.5. Fabrication of Silver NP Cages. For the fabrication of silver NP cages, the capsule suspension was incubated in an incubator shaker for 1 h at 80 °C, near the pK_a value of DS (pH 2). The resulting silver micro/nanocages were washed three times with deionized water and were used for further studies.

2.6. Catalytic Activity. The epoxidation reaction was carried out in a 25 mL round-bottom flask immersed in a water bath. The experimental set up was equipped with a condenser, thermometer, and nitrogen balloon to control the reaction conditions. In a typical reaction, 10 mmol of the substrate, 10 mmol of TBHP (70%, toluene solution), 5 mL of acetonitrile, and 0.2 mmol of cycloheptanone (internal standard) were homogenized via magnetic stirring and the mixture was heated to 65 °C. Next hollow silver cages (20 wt % of the substrate) were added with vigorous stirring and the condenser was effectively cooled by circulation of ice-cooled water. The reaction products were analyzed on a Shimadzu 14B gas chromatograph equipped with an OV-1 capillary column fitted with a FID detector. Reaction products were identified using authentic compounds and unreacted peroxides were estimated through potentiometric titration with a Ce^{4+} solution.

2.7. Other Characterization. For scanning electron microscopy (SEM) analysis, a drop of the capsule/cage suspension was placed on a silicon wafer and air-dried overnight to remove the moisture completely. After sputtering a thin gold layer, the samples were analyzed using a field emission scanning electron microscope (FEI-SIRION, Eindhoven, Netherlands). Field emission transmission electron microscopy (FE-TEM) measurements were performed on a Tecnai F30 (FEI, Eindhoven, The Netherlands) microscope operating at 200 kV. For atomic force microscopy (AFM) analysis, a drop of capsule suspension was placed on a silicon wafer and air-dried overnight. Then the samples were characterized using a Nanosurf Easy Scan2 AFM (Nanoscience Instruments Inc., U.S.A.) in air at room temperature by contact mode. To calculate the average size of silver NPs, 500 NPs were selected stochastically from SEM images and their average size and standard deviation were calculated by ImageJ software. For Fourier transform infrared (FTIR) analysis, dried cages prior to and after layer dissolution were mixed with KBr powder and made into pellets. Spectra were acquired in transmission mode on a Nicolet 5700 FTIR spectrometer (Thermo Electron Corporation, U.S.A.). UV−visible (UV−vis) spectra of the NP cage suspensions were recorded using a T60 UV−vis spectrophotometer (PG Instruments Ltd., U.K.).

3. RESULTS AND DISCUSSION

Engineering the structure of nanomaterials enables control of their physical and chemical properties and enhances their performance for given applications, such as catalysis. Herein, we demonstrate the synthesis of silver nanocages based on LbL assembly. The present strategy involves two steps: (1) alternate adsorption of PAH and DS on a silica template and (2) in situ synthesis of silver NPs, followed by selective core and layer component dissolution as shown in Figure 1. Polyelectrolytes

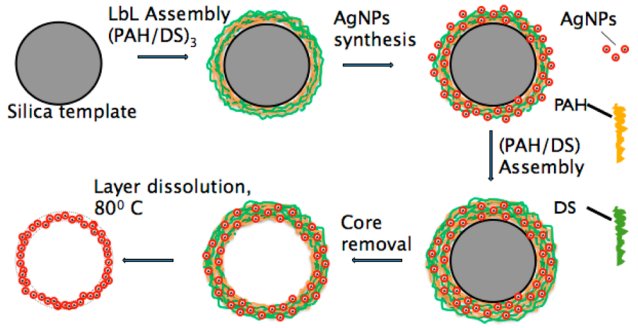

Figure 1. Schematic representation of the fabrication of NP cages.

like DS, which bears sulfonate groups in its polymeric backbone, are attractive since they have higher affinities with silver ions (Ag^+).[16] When DS is assembled over a silica template, sulfonate groups attract Ag^+ ions from the suspension and can be subsequently reduced to Ag(0) NPs in the presence of PEG. PEG acts as a reducing and stabilizing agent for the reduction process.[18] The template dissolution after NP synthesis generally results in polyelectrolyte capsules with newly formed silver NPs in the shell.[19] An intrinsic property of LbL capsules is that they can be disassembled near the pK_a values of the layer constituents, as the pH-induced imbalance of the charges overpowers the attractive polymer−polymer interactions. By using this property, we selectively leached out the layer components (PAH/DS) to obtain silver

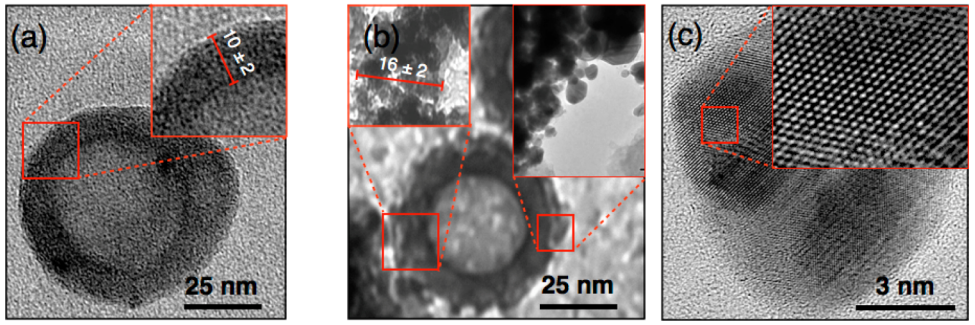

Figure 2. TEM images show the morphology of polyelectrolyte nanocapsules and nanocages. (a) Nanocapsule, (b) nanocage, and (c) HR-TEM lattice fringes of silver NPs present in the cage shell. Insets in the images show a magnified image of the marked area of the capsule or cage. Silica NPs were used as templates for nanocage preparation.

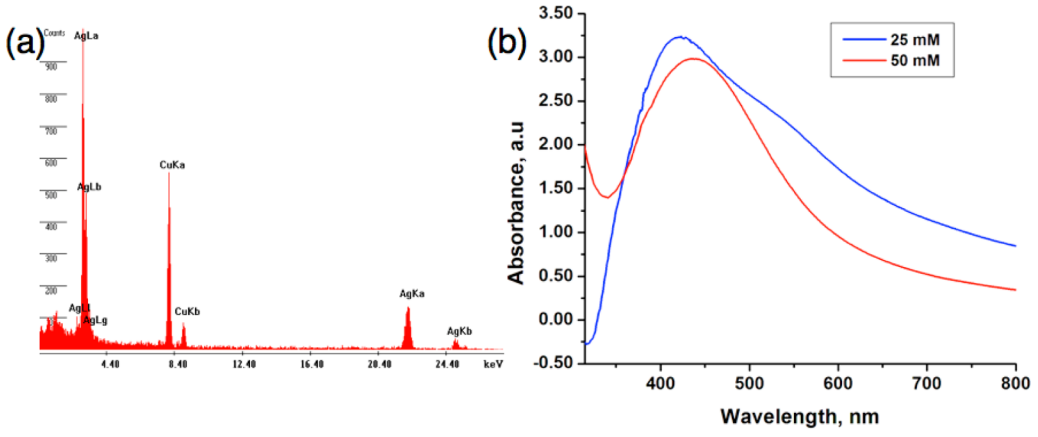

Figure 3. (a) EDX spectrum and (b) UV–vis spectra of silver nanocages.

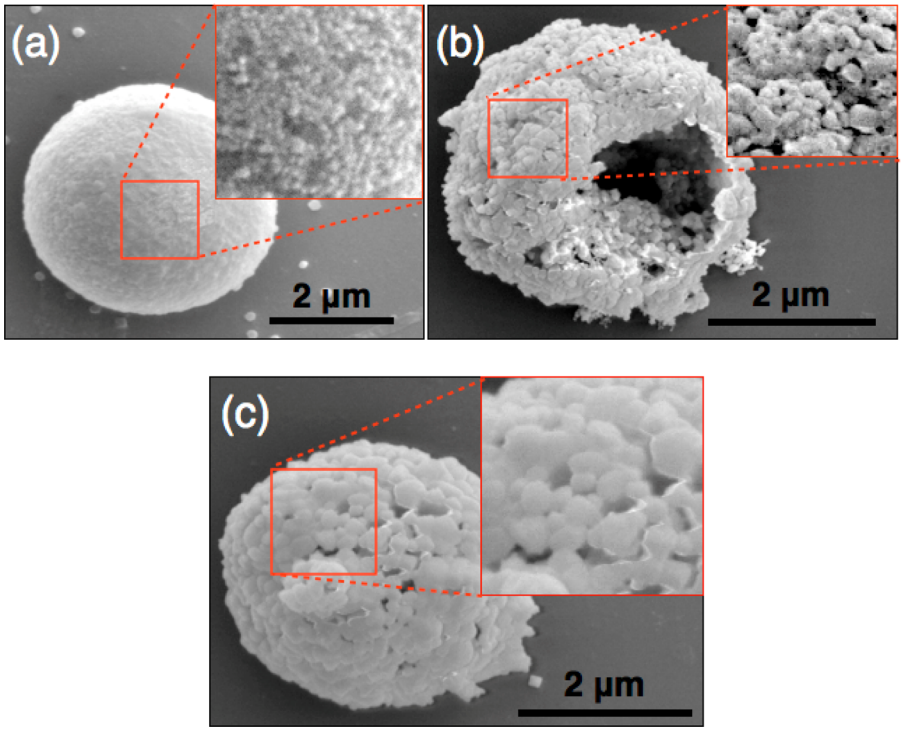

Figure 4. SEM images show the morphology of coated silica particles and microcages as a function of $AgNO_3$ concentration. (a) PAH/DS-coated silica particle with synthesized Ag NPs at 25 mM $AgNO_3$ and fabricated Ag NP microcages with (b) 25 and (c) 50 mM $AgNO_3$. Inset in the image shows the magnified image of the coated particle or microcage. Silica microparticles of 4.27 ± 0.25 μm were used for cage preparation.

dx.doi.org/10.1021/am500229v | ACS Appl. Mater. Interfaces 2014, 6, 3275−3281

nanocages. The resulting hollow silver NP cage constituted with silver NP building blocks is shown in Figure 2. The capsules (without NPs) appeared smooth and thin since only polyelectrolytes were present in their shell (Figure 2a). The average capsule size and thickness were 80 ± 10 nm and 10 ± 2, respectively. A notable contrast difference between the shell and interior of the capsules implied the hollowness of the capsule. On the other hand, hollow NP cages showed a rough surface morphology when compared to normal capsules (Figure 2b) because of the presence of silver NPs, which were arranged randomly, in the capsule wall after layer dissolution at 80 °C. During this process, the size of the hollow cage decreased from 80 ± 10 to 55 ± 10 nm. The difference in capsule size was attributed to the layer dissolution and temperature-induced shrinking of the capsules.[20] Notably, the average wall thickness during this process increased from 10 ± 2 nm to 16 ± 2 nm. Spherical NPs of approximately 5 ± 2 nm could be seen clearly in the walls of the hollow NP cages (Figure 2b insets). These silver NP cages were investigated with energy dispersive X-ray spectroscopy (EDX) as shown in Figure 3a. The presence of silver peaks in the EDX spectrum confirmed the presence of silver NPs in the shell.

The formed cages were investigated by UV spectroscopy, which has proven to be a very sensitive method for monitoring the formation of silver NPs because of the appearance of a surface plasmon absorption band. Figure 3b shows the absorption spectrum of nanocages synthesized at 25 and 50 mM $AgNO_3$, respectively. Absorption bands in the range of 380−500 nm were attributed to the collective oscillation of the electron gas in nanoscale particles.[18] An absorption band was observed for both samples, which confirmed the presence of silver NPs. Furthermore, it is important to note that the λ_{max} red-shifted when the $AgNO_3$ concentration was increased from 25 to 50 mM. This confirmed the formation of larger silver NPs at a higher $AgNO_3$ concentration. It is believed that an increased number of silver ions can promote particle growth during NP synthesis.

To understand the influence of $AgNO_3$ concentration on NP formation, arrangement, and cage morphology, the procedure was repeated with micrometer-sized cages and was investigated systematically by scanning electron microscope (SEM). Figure 4a shows the polyelectrolyte (PAH/DS)-coated silica particles (4.27 ± 0.25 μm) with silver NPs in the shell. The NPs were uniformly formed on the PAH/DS-coated particles. When the core and layer components were leached out, the particle transformed into a hollow cage with a shell domain comprised of only silver NPs. Silver NPs of 20 ± 5 nm were arranged on the cage surface. The interparticle pores were also clearly seen, confirming the hollowness of the cages (Figure 4b and c). When the $AgNO_3$ concentration was increased from 25 to 50 mM, the NP size increased from 20 ± 5 to 40 ± 5 nm. At the higher $AgNO_3$ concentration, more silver cations were available to participate in the ion exchange with PEG. This result corroborated well with the UV−visible data, which suggested that the NP size increased as a function of $AgNO_3$ concentration.

FTIR spectroscopy was used to investigate the layer dissolution process. Figure 5 shows the FTIR spectrum of the nanocages prior to and after the layer dissolution process. Sulfonate groups were identified by the symmetric and asymmetric vibrations of the (S═O) and (O−S−O) functionalities. The spectrum of the capsules before the dissolution process showed four notable peaks at about 1192, 1005, 824, and 570 cm^{-1}, which corresponded to the symmetric and asymmetric vibrations of the (S═O) and (O−S−O) groups, respectively.[21−23] The peaks at 1633 and 3443 cm^{-1} corresponded to the N−H bending (scissoring) vibrations of PAH and O−H vibrations, respectively.[21,22] These bands indicated the presence of PAH and DS prior to dissolution. However, after the dissolution process, the vibration bands of (S═O) and (O−S−O) groups were not clearly observed. This result confirmed that the layer components were successfully leached out from the capsule surface and resulting cages.

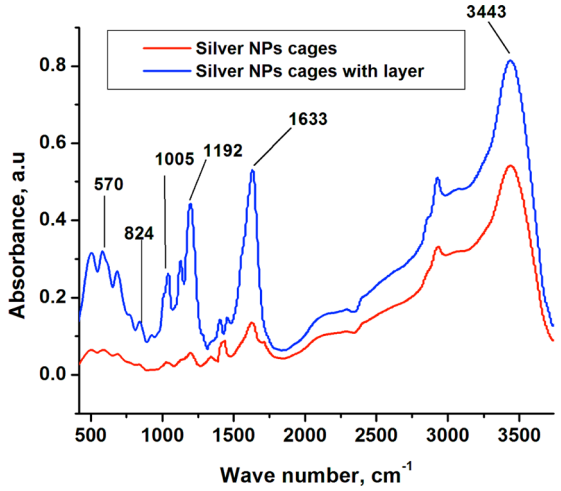

Figure 5. FTIR spectra of nanocages prior to and after layer dissolution process.

The success of this layer leach-out methodology could be correlated with the properties of the polysaccharides and polyelectrolytes. Polyelectrolyte capsules composed of DS undergo two types of physicochemical changes near their pK_a values at higher temperatures: (1) protonation of the sulfonate groups of DS which induces repulsion in the polymeric network followed by swelling of the capsule[24,25] and (2) increased polyelectrolyte capsule thickness at the expense of decreasing diameter.[20,26] Both processes oppose each other and their balance yields intact hollow cages. To investigate these processes, the morphological changes of the capsules were analyzed as a function of temperature and pH. When the layer components were dissolved at room temperature (pH 2), the structures could not retain their shape and they appeared like a cluster of NPs (Figure 6a). A possible explanation for this phenomenon might be the faster diffusion of DS molecules from the hollow silver cages. Polyelectrolyte capsules swell at acidic pH values because of phase segregation upon protonation of the sulfonate groups.[24,25] The swelling, which is due to the transformation of the sulfonate groups of DS from the dissociated to associated state, destabilizes the interaction between the polyelectrolytes (PAH/DS) and causes the resulting structure to collapse. On the other hand, the cages were subject to wall thickening and densification with a significant size reduction when treated at neutral pH at 80 °C (Figure 6b). Notably, the cages exhibited a full spherical morphology instead of that of collapsed conventional polyelectrolyte capsules. At a high magnification, the shell morphology displayed a wavy structure with patterned peaks and valleys. The central core cavity obtained by core removal could also be seen clearly on the surface, confirming the hollow cage structure. These results corroborated well with previous reports suggesting that polyelectrolyte capsules undergo wall

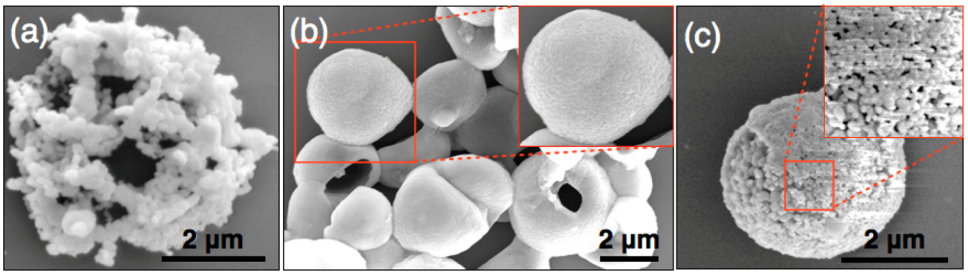

Figure 6. SEM images show the morphology of the capsules and cages after layer dissolution under different conditions. Layer dissolution performed at (a) pH 2 at room temperature, (b) pH 7 at 80 °C, and (c) pH 2 at 80 °C. Silica microparticles of 4.27 ± 0.25 μm were used for cage preparation.

densification and thickening at the expense of their diameter.[20,26] The wall densification and shrinkage enabled the collapsed structure to swell and attain a fully formed spherical structure.

The characteristic features of these two processes could be successfully combined to yield intact hollow cages when layer dissolution was performed at pH 2 and 80 °C. The successfully obtained hollow cages made of fine silver NPs are shown in Figure 6c. The cage was uniformly arranged with silver NPs and the interparticle pores were also clearly seen. We believe that an equilibrium was established between these two processes when the dissolution was performed at a higher temperature near the pK_a value. The dissolution of DS was slowed by the shell thickening and densification at higher temperatures. This favors cage formation in two ways: (1) phase segregated DS molecules diffuse slowly into the bulk solution and provide enough time for the shells to realign themselves and (2) temperature-induced shrinking brings the NPs closer together and forces contact between them, thus enabling the cages to maintain their shape after layer dissolution. Therefore, by maintaining the balance between these two processes, we successfully leached out the layer components and produced the MNP cages.

Preliminary experiments were also performed with planar glass substrates. With this methodology, we could successfully generate patterned silver NPs on the planar glass substrates as shown in Supporting Information (Figure S6).

Recently, many transition-metal NPs have been utilized in various liquid-phase reactions because of their very high surface area. Nanoparticles of noble metals such as Pt and Pd have been used as catalysts for olefin hydrogenation and in carbon−carbon coupling reactions, including Heck and Suzuki reactions.[27,5] Herein, we report the oxidation properties of silver NP cages using tert-butylhydroperoxide (TBHP) as an oxidant under liquid-phase conditions.

3.1. Catalytic Activity of Cages. We investigated the oxidation properties of the produced cages using TBHP as an oxidant under liquid-phase conditions. A typical epoxidation reaction using the silver cage structures is depicted in Scheme 1. As illustrated in Table 1, the silver nanocages exhibited a very high activity in the epoxidation of different cyclic and acylic olefins. Epoxidation of styrene (entry 1) gave the corresponding epoxide in a high yield (79.6%), and the major side product, phenylacetaldehyde (19.2%), was produced by the rearrangement of the primary epoxide product according to literature reports.[28−30] Entries 2−4 show the reactivities of cyclic olefins to produce the corresponding cycloolefin oxide, 1,2-cycloalkane diol, and allylic oxidation products (2-cycloolefin-1-one and 2-cycloolefin-1-ol). All cyclic olefins showed a very high selectivity for epoxides and the observed reactivity pattern of different cyclic olefins suggested that hollow nanocages allowed a smooth diffusion and interaction of the reactants and/or products on the surface of the silver cages. Acylic olefins like 2-hexene and 2-octene (entries 5 and 6) also produced the respective epoxides and diols as the major products. Entry 7 shows the reactivity of cyclohexene at a high concentration of TBHP (substrate/TBHP = 1:2), which marginally improved the conversion level. Similar to other metallic nanoparticles, the silver cage structures have a characteristic high surface-to-volume ratio vis-à-vis surface area. Hence, a large number of silver atoms are present at the surface and take part in the catalysis. Although there are many reports regarding the epoxidation of lower alkenes such as ethylene, propylene, and butene using silver catalysts,[31−34] no epoxidation reaction has been carried out with higher alkenes using a silver/TBHP catalytic system. Further, the Ag-cage structures exhibited better epoxide selectivity compared to titanium silicate-based catalysts.[29] In order to reuse the silver catalysts, the cages were activated with 5% H_2 diluted with nitrogen at 140 °C for 2 h. The activated catalyst was tested for recyclability and entry 8 exhibits the activity of the silver cages after 4 successive reuses, demonstrating the true heterogeneous nature of the catalytic

Table 1. Epoxidation of Olefins to Epoxides[a]

			product distribution (%)		
no.	substrates	conversion (%)	epoxide	diol	others
1	styrene	81.7	79.6	1.2	19.2[b]
2	cyclohexene	79.3	83.0	9.5	7.5
3	cyclooctene	70.8	89.0	7.3	3.7
4	cyclododecene	75.4	85.4	8.7	5.9
5	2-hexene	69.1	88.5	10.1	1.4
6	2-octene	62.8	87.0	11.1	1.9
7[c]	cyclohexene	82.3	81.4	12.3	6.3
8[d]	cyclohexene	74.8	84.6	9.8	5.6
9[e]	styrene	68.4	82.6	8.3	9.1

[a]Reaction conditions: 10 mmol substrate, 10 mmol TBHP, 5 mL of acetonitrile, 0.2 mmol cycloheptanone, reaction temperature 65 °C, reaction time 4 h. Twenty weight percent catalysts with respect to substrates. [b]Phenylacetaldehyde. [c]Substrate/TBHP = 1: 2. [d]Catalytic activity after 4 successive uses. "Others" refers to allylic oxidation products. [e]Catalytic activity of micrometer sized silver cages.

Scheme 1. Epoxidation of Styrene to Styrene Epoxide

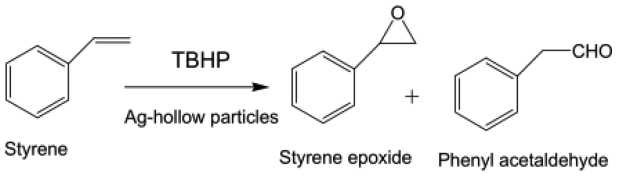

dx.doi.org/10.1021/am500229v | ACS Appl. Mater. Interfaces 2014, 6, 3275−3281

system. There was no significant change in morphology after four successive uses (Supporting Information; Figure S7). A possible epoxidation mechanism involves the interaction of TBHP on the silver nanocages to give electrophilic oxygen atoms on the silver surface which attack the −C═C− to yield the epoxides.[35−37] It is also possible that Ag nanoparticles with high surface areas and surface energies can improve the epoxidation reaction through a lower activation energy.

CONCLUSION

We report a methodology to prepare silver NP cages by selectively dissolving outer layer components from the LbL-assembled capsules. Spherical NPs of 5 ± 2 nm could be seen clearly in the cage shell. The size of the NPs increased to 20 ± 5 nm when the nanosized template was replaced with a micrometer-sized template. Heat treatment of polyelectrolyte capsules near their pK_a values enabled an equilibrium to be established between the temperature-induced shrinking and protonation-induced swelling and facilitated the removal of the layer components. These cages showed a very high catalytic activity in the epoxidation of olefins and could be reused at least four times without any compromise in their activity. Notably, the approach demonstrated here illustrates the potential for the development of metal NP cages and may offer a promising catalytic system for the epoxidation of olefins.

ASSOCIATED CONTENT

Supporting Information

SEM, TEM, HR-TEM, and AFM images shwoing the morphology and structures described in this work. This information is available free of charge via the Internet at http://pubs.acs.org/.

AUTHOR INFORMATION

Corresponding Author

*E-mail: rsanandhakumar@gmail.com.

Notes

The authors declare no competing financial interest.

ACKNOWLEDGMENTS

The authors would like to thank the Institute Nanoscience Initiative, Indian Institute of Science (IISc) for access to the microscopy facility.

REFERENCES

(1) Anandhakumar, S.; Raichur, A. M. Polyelectrolyte/Silver Nanocomposite Multilayer Films as Multifunctional Thin Film Platforms for Remote Activated Protein and Drug Delivery. *Acta Biomater.* **2013**, *9*, 8864−8874.

(2) Radziuk, D.; Shchukin, D. G.; Skirtach, A.; Möhwald, H.; Sukhorukov, G. Synthesis of Silver Nanoparticles for Remote Opening of Polyelectrolyte Microcapsules. *Langmuir* **2007**, *23*, 4612−4617.

(3) Chen, X.; Mao, S. S. Titanium Dioxide Nanomaterials: Synthesis, Properties, Modifications, and Applications. *Chem. Rev.* **2007**, *107*, 2891−2959.

(4) Lou, X. W.; Archer, L. A. A General Route to Nonspherical Anatase TiO_2 Hollow Colloids and Magnetic Multifunctional Particles. *Adv. Mater.* **2008**, *20*, 1853−1858.

(5) Kim, S.-W.; Kim, M.; Lee, W. Y.; Hyeon, T. Fabrication of Hollow Palladium Spheres and Their Successful Application to the Recyclable Heterogeneous Catalyst for Suzuki Coupling Reactions. *J. Am. Chem. Soc.* **2002**, *124*, 7642−7643.

(6) Caruso, F. Nanoengineering of Particle Surfaces. *Adv. Mater.* **2001**, *13*, 11−22.

(7) Mulvaney, P.; Giersig, M.; Ung, T.; Liz-Marzan, L. M. Direct Observation of Chemical Reactions in Silica-Coated Gold and Silver Nanoparticles. *Adv. Mater.* **1997**, *9*, 570−575.

(8) Guo, X. C.; Dong, P. Multistep Coating of Thick Titania Layers on Monodisperse Silica Nanospheres. *Langmuir* **1999**, *15*, 5535−5540.

(9) Radtchenko, I. L.; Sukhorukov, G. B.; Gaponik, N.; Kornowski, A.; Roach, A. L.; Möhwald, H. Core−Shell Structures Formed by the Solvent-Controlled Precipitation of Luminescent CdTe Nanocrystals on Latex Spheres. *Adv. Mater.* **2001**, *13*, 1684−1687.

(10) Keller, S. W.; Johnson, S. A.; Brigham, E. S.; Yonemoto, E. H.; Mallouk, T. E. Photo Induced Charge Separation in Multilayer Thin Films Grown by Sequential Adsorption of Polyelectrolytes. *J. Am. Chem. Soc.* **1995**, *117*, 12879−12880.

(11) Sasidharan, M.; Nakashima, K.; Gunawardhana, N.; Yokoi, T.; Inoue, M.; Yusa, S.-I.; Yoshio, M.; Tatsumi, T. Novel Titania Hollow Nanospheres of Size 28 ± 1 nm Using Soft-Templates and Their Application for Lithium-Ion Rechargeable Batteries. *Chem. Commun.* **2011**, *47*, 6921−6923.

(12) Lu, W.; Wang, W.; Su, Y.; Li, J.; Jiang, L. Formation of Polydiacetylene−NH_2−Gold Hollow Spheres and Their Ability in DNA Immobilization. *Nanotechnology* **2005**, *16*, 2582−2586.

(13) Zhang, X.; Li, D. Metal-Compound-Induced Vesicles as Efficient Directors for Rapid Synthesis of Hollow Alloy Spheres. *Angew. Chem.* **2006**, *118*, 6117−6120.

(14) Caruso, F.; Spasova, M.; Susha, A.; Giersig, M.; Caruso, R. A. Magnetic Nanocomposite Particles and Hollow Spheres Constructed by a Sequential Layering Approach. *Chem. Mater.* **2001**, *13*, 109−116.

(15) Caruso, F.; Caruso, R. A.; Möhwald, H. Production of Hollow Microspheres from Nanostructured Composite Particles. *Chem. Mater.* **1999**, *11*, 3309−3314.

(16) Anandhakumar, S.; Raichur, A. M. A Facile Route to Synthesize Silver Nanoparticles in Polyelectrolyte Capsules. *Colloids Surf., B* **2011**, *84*, 379−383.

(17) Stober, W.; Fink, A. Controlled Growth of Monodisperse Silica Spheres in the Micron Size Range. *J. Colloid Interface Sci.* **1968**, *26*, 62−69.

(18) Luo, C.; Zhang, Y.; Zeng, X.; Zeng, Y.; Wang, Y. The Role of Poly(ethylene glycol) in the Formation of Silver Nanoparticles. *J. Colloid Interface Sci.* **2005**, *288*, 444−448.

(19) Anandhakumar, S.; Vijayalakshmi, S. P.; Jagadeesh, G.; Raichur, A. M. Silver Nanoparticle Synthesis: Novel Route for Laser Triggering of Polyelectrolyte Capsules. *ACS Appl. Mater. Interfaces* **2011**, *3*, 3419−3424.

(20) Köhler, K.; Sukhorukov, G. B. Heat Treatment of Polyelectrolyte Multilayer Capsules: A Versatile Method for Encapsulation. *Adv. Funct. Mater.* **2007**, *17*, 2053−2061.

(21) Beyer, S.; Bai, J.; Blocki, A. M.; Kantak, C.; Xue, Q.; Raghunath, M.; Trau, D. Assembly of Biomacromolecule Loaded Polyelectrolyte Multilayer Capsules by Using Water Soluble Sacrificial Templates. *Soft Matter* **2012**, *8*, 2760−2768.

(22) Cakić, M.; Nikolić, G.; Ilić, L.; Stanković, S. Synthesis and FTIR Characterization of Some Dextran Sulphates. *Chem. Ind. Chem. Eng. Q.* **2005**, *1*, 74−78.

(23) Rosca, C.; Novac, O.; Lisa, G.; Popa, M. I. Polyelectrolyte Complexes of Chitosan with Dextran Sulphate: Synthesis and Characterization. *Cell. Chem. Technol.* **2011**, *45*, 185−189.

(24) Mauser, T.; Dejugnat, C.; Mohwald, H.; Sukhorukov, G. B. Microcapsules Made of Weak Polyelectrolytes: Templating and Stimuli-Responsive Properties. *Langmuir* **2006**, *22*, 5888−5893.

(25) Anandhakumar, S.; Nagaraja, V.; Raichur, A. M. Reversible Polyelectrolyte Capsules as Carriers for Protein Delivery. *Colloids Surf., B* **2010**, *78*, 266−274.

(26) Gao, C.; Leopardi, S.; Moya, S.; Donath, E.; Möhwald, H. Swelling and Shrinking of Polyelectrolyte Microcapsules in Response to Changes in Temperature and Ionic Strength. *Chem.—Eur. J.* **2003**, *9*, 915−920.

(27) Reetz, M. T.; Westermann, E. Phosphane-Free Palladium-Catalyzed Coupling Reactions: The Decisive Role of Pd Nanoparticles. *Angew. Chem., Int. Ed.* **2000**, *39*, 165−168.

(28) Laha, S. C.; Kumar, R. Selective Epoxidation of Styrene to Styrene Oxide over TS-1 Using Urea-Hydrogen Peroxide as Oxidizing Agent. *J. Catal.* **2001**, *204*, 64−70.
(29) Sasidharan, M.; Bhaumik, A. Novel and Mild Synthetic Strategy for the Sulfonic Acid Functionalization in Periodic Mesoporous Ethylene-Silica. *ACS Appl. Mater. Interfaces* **2013**, *5*, 2618−2625.
(30) Sasidharan, M.; Wu, P.; Tatsumi, T. Epoxidation of α,β-Unsaturated Carbonyl Compounds over Various Titanosilicates. *J. Catal.* **2002**, *205*, 332−338.
(31) Ozbek, M. O.; Onal, I.; Van Santen, R. A. Why Silver is the Unique Catalyst for Ethylene Epoxidation. *J. Catal.* **2011**, *284*, 230−235.
(32) Lambert, R. M.; Williams, F. J.; Cropley, R.; Palermo, A. Heterogeneous Alkene Epoxidation: Past, Present and Future. *J. Mol. Catal. A: Chem.* **2005**, *228*, 27−33.
(33) Linic, S.; Barteau, M. A. Control of Ethylene Epoxidation Selectivity by Surface Oxametallacycles. *J. Am. Chem. Soc.* **2003**, *125*, 4034−4035.
(34) Christopher, P.; Linic, S. Engineering Selectivity in Heterogeneous Catalysis: Ag Nanowires as Selective Ethylene Epoxidation Catalysts. *J. Am. Chem. Soc.* **2008**, *130*, 11264−11265.
(35) Grant, R. B.; Lambert, R. M. A Single Crystal Study of the Silver-Catalysed Selective Oxidation and Total Oxidation of Ethylene. *J. Catal.* **1985**, *92*, 364−375.
(36) Linic, S.; Barteau, M. A. Construction of a Reaction Coordinate and a Microkinetic Model for Ethylene Epoxidation on Silver from DFT Calculations and Surface Science Experiments. *J. Catal.* **2003**, *214*, 200−212.
(37) Pulido, A.; Concepcion, P.; Boronat, M.; Corma, A. Aerobic Epoxidation of Propene over Silver (1 1 1) and (1 0 0) Facet Catalysts. *J. Catal.* **2012**, *292*, 138−147.